Carbohydrate Polymers 98 (2013) 1497–1504

Contents lists available at ScienceDirect

Carbohydrate Polymers

journal homepage: www.elsevier.com/locate/carbpol

Fabrication and characterisation of α-chitin nanofibers and highly transparent chitin films by pulsed ultrasonication

Yun Lu [a], Qingfeng Sun [a], Xilin She [b], Yanzhi Xia [b], Yixing Liu [a], Jian Li [a,*], Dongjiang Yang [b,**]

[a] Material Science and Engineering College, Key Laboratory of Bio-based Material Science and Technology, Ministry of Education, Northeast Forestry University, Harbin 150040, PR China
[b] College of Chemistry, Chemical and Environmental Engineering, Qingdao University, Qingdao 266071, PR China

ARTICLE INFO

Article history:
Received 25 February 2013
Received in revised form 14 July 2013
Accepted 16 July 2013
Available online 24 July 2013

Keywords:
Chitin nanofiber
Ultrasonic
Transparent
Film
Foam

ABSTRACT

α-Chitin nanofibers were fabricated with dried shrimp shells *via* a simple high-intensity ultrasonic treatment under neutral conditions (60 KHz, 300 W, pH = 7). The diameter of the obtained chitin nanofibers could be controlled within 20–200 nm by simply adjusting the ultrasonication time. The pulsed ultrasound disassembled natural chitin into high-aspect-ratio nanofibers with a uniform width (19.4 nm after 30 min sonication). The EDS, FTIR, and XRD characterisation results verified that α-chitin crystalline structure and molecular structure were maintained after the chemical purification and ultrasonic treatments. Interestingly, ultrasonication can slightly increase the degree of crystallinity of chitin (from 60.1 to 65.8). Furthermore, highly transparent chitin films (the transmittance was 90.2% at a 600 nm) and flexible ultralight chitin foams were prepared from chitin nanofiber hydrogels.

1. Introduction

Natural polymers are much more attractive than artificial polymers due to their "green" characteristics, such as biodegradability, biocompatibility, renewability, and sustainability (Ifuku & Saimoto, 2012), and are more suitable for controlled drug release formulations, cosmetics, food presentation, fertilisers, tissue engineering (Lu et al., 2012; Muzzarelli, 2009; Watthanaphanit, Supaphol, Tamura, Tokura, & Rujiravanit, 2008), and biodegradable packaging materials (Synowiecki & Al-Khateeb, 2003). Therefore, the production of nanofibers with natural polymers, namely, cellulose and chitin, has received increasing attention (Ding et al., 2012; Ifuku & Saimoto, 2012; Ifuku et al., 2009; Muzzarelli et al., 2007; Qin, Lu, Sun, & Rogers, 2010; Zeng, He, Li, & Wang, 2011). However, in arthropod exoskeletons, chitin microfibrils are embedded in protein and minerals (Chen, Lin, McKittrick, & Meyers, 2008). Thus, effective methods to extract nanofibers from biomass directly are highly desirable. And it is necessary to develop a facile approach to synthesising natural nanofibers without changing their chemical structures. Among the variety of existent approaches, the utilisation of ultrasound for materials synthesis has been extensively examined for many years and is now one of the most powerful tools in nanostructured materials synthesis (Bang & Suslick, 2010; Zeiger & Suslick, 2011). The chemical effects of ultrasound are caused by acoustic cavitation, which generates localised hot spots with very high temperatures (>5000 K), pressures (>20 MPa), and heating/cooling rates (>10^{10} K/s) (Suslick, 1990). Such extreme environments provide a unique platform to break the strong cellulose interfibrillar hydrogen bonding, allowing nanofibers to be gradually disintegrated (Cheng, Wang, & Han, 2010; Tischer, Sierakowski, Westfahl, & Tischer, 2010; Zhao, Feng, & Gao, 2007). Furthermore, this isolation method may be universally applicable to all the biomass resources consisting of nanofibers and other embedding matrixes. Accordingly, this study investigates the extraction of natural α-chitin nanofibers from prawn shells under pulsed ultrasonication.

Chitin is the second most abundant polysaccharide after cellulose. It occurs in arthropods, mollusks, and fungi. Chitin is synthesised *in vivo* as an amorphous aminopolysaccharide ready to be linked to proteins; as a consequence, isolated chitin is the partly (*ca.* 10%) deacetylated (1-4)-2-acetamido-2-deoxy-β-D-glucan (Muzzarelli, 2011; Muzzarelli et al., 2012). Unfortunately, most chitin is discarded as a by-product of the food industry (mainly shrimp and crab shells) without effective utilisation. Therefore, it is important to develop efficient methods for the exploitation of this resource.

* Corresponding author at: Northeast Forestry University, No. 26 Hexing Road, Xiangfang District, Harbin 150040, PR China. Tel.: +86 451 82192399; fax: +86 451 82192399.
** Corresponding author.
E-mail addresses: jianli@nefu.edu.cn (J. Li), d.yang@qdu.edu.cn (D. Yang).

0144-8617/$ – see front matter © 2013 Elsevier Ltd. All rights reserved.
http://dx.doi.org/10.1016/j.carbpol.2013.07.038

Chitin chains tend to be connected by both hydrogen bonds and Van der Waals forces, forming a microfibril structure. Native chitins in crustacean shells are also highly crystalline and are arranged in an antiparallel fashion as α-chitin microfibrils. These microfibrils consist of nanofibrils with diameters of 2–5 nm and lengths of ~300 nm embedded in a protein matrix (Chen et al., 2008; Giraud-Guille, 1984; Raabe et al., 2006). The presence of nanofibrils suggests that chitin is a good candidate for biomass nanofibers. However, it is generally difficult to convert chitins into individual chitin fibres with uniform widths dispersed in water at the nano-fibril level because the chitin fibrils are tightly bound to each other through a large number of hydrogen bonds in living systems. To obtain chitin nanofibers with high aspect ratios and uniform width from arthropod exoskeletons, various methods have been employed, such as the use of grinders (Ifuku et al., 2009), high-speed blending (Shams, Ifuku, Nogi, Oku, & Yano, 2011), TEMPO-mediated oxidation (Isogai, Saito, & Fukuzumi, 2011; Muzzarelli, Muzzarelli, Cosani, & Terbojevich, 1999), and partial deacetylation (Fan, Saito, & Isogai, 2010). However, compared with the numerous reports on the preparation of cellulose nanofibers, few have reported on the preparation of chitin nanofibers with a top-down approach.

Herein, we report the successful nano-fibrillation of chitin from prawn shells using facile pulsed ultrasonication, yielding high-crystallinity, high-quantity chitin nanofibers with widths of ~20 nm. This high-intensity ultrasonication treatment can separate nanofibers from natural nanofiber-embedding matrixes after the removal of the matrix substances. More interestingly, the obtained width-uniform nanofibers can directly form highly optical transparent films. This neat bio-nanofiber material is the perfect candidate for continuous roll-to-roll processing in the future production of electronic devices. In addition, ultralight and flexible chitin nanoporous foams are prepared from uniform-width nanofibers using freezing drying.

2. Materials and methods

2.1. Raw materials

Fresh *Penaeus monodon* (black tiger prawn) prawn shells were collected from Queensland, Australia. All prawns were carefully peeled to remove obvious meat and retain the back and tail. These materials were washed three times with tap water, air-dried, and sieved through a 60-mesh sieve. The ground shells were used as a source of chitinous biomass fibres. Practical-grade chitin was purchased from Aladdin. Ethanol, sodium chlorite, acetic acid, potassium hydroxide, hydrochloric acid, *t*-butyl alcohol (*t*-BuOH), and other chemicals were of laboratory grade and used without further purification.

2.2. Purification of chitin by removing matrix components

The dried fresh prawn shells were purified to prepare the predecessor of chitin nanofibers. First, approximately 2 g of the prawn shells were immersed in a Soxhlet apparatus with 95% ethanol at 80 °C for 6 h under reflux to remove pigment and lipid compositions, after which the prawn shells were rinsed with water. The prawn shells were then treated with an acidified sodium chlorite solution (1.5 wt% $NaClO_2$, buffered to pH 4.0) at 80 °C for 5 h. The samples were treated in 5 wt% KOH at 90 °C for 2 h and then in 3.6 wt% HCl solutions at 80 °C for 2 h to remove proteins and mineral salts, such as calcium carbonates (Fig. 1). These treatment steps with acid and alkali were repeated 3 times, followed by filtration and washing with distilled water. Because the drying of chitin fibres generates strong hydrogen bonds between fibres, chitin must be kept wet after purification for the next nanofibrillation (Abe, Iwamoto, & Yano, 2007; Ifuku et al., 2009).

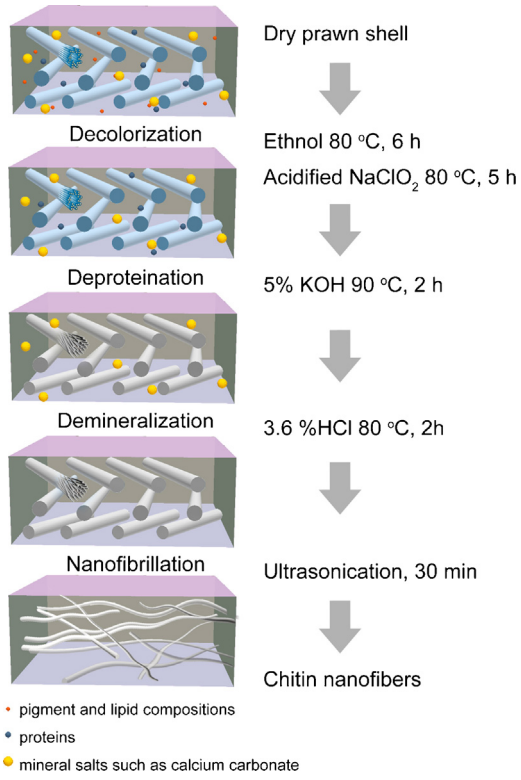

Fig. 1. Experimental procedure for individualising α-chitin nanofibers from prawn shells.

2.3. Ultrasonic nanofibrillation of chitin

To facilitate nanofibrillation, the purified wet chitin was dispersed in water such that approximately 400 mL of the water slurry contained 0.5 wt% sample. Sonication was performed at 60 kHz with a Sonifiers® Cell Disruptor/Homogeniser (S450D, Branson Ultrasonics Corp.) with a 1-cm^2-diameter titanium horn. The subsequent ultrasonication experiments were performed under a 50% duty cycle (*i.e.*, a repeating cycle of 0.5-s ultrasonic treatment and 0.5-s shutdown) to reduce temperature variation and were conducted for 30 min with an output power of 300 W to isolate the fibres. Ultrasonic treatment was carried out in an ice/water bath, and ice was maintained throughout the entire ultrasonication. A water suspension containing chitin nanofibers was obtained after centrifugation (5000 rpm, 5 min).

2.4. Fabrication of neat film and foams with chitin nanofibers

The suspension was subjected to dialysis tubing cellulose membrane (avg. flat width = 76 mm, molecular weight cut-off = 14,000, Sigma–Aldrich), which was hung vertically in a clean place with good ventilation. With the loss of water molecules, the volume of the suspension was reduced by two thirds after 48 h. A concentrated suspension was collected at the bottom of the dialysis, containing ~1.5 wt% nanofibers and exhibiting a high viscosity with a gel-like appearance. Some of this hydrogel was subjected to solvent-exchange with *t*-BuOH, after which the nanofibers (chitin) organogel containing *t*-BuOH and the other chitin hydrogel were freeze-dried at −55 °C and vacuum-dried for 24 h at 25 μPa. Chitin foams were obtained. The remaining dialysis membrane was carefully liberated and filled with water in a tank. A thin chitin wet

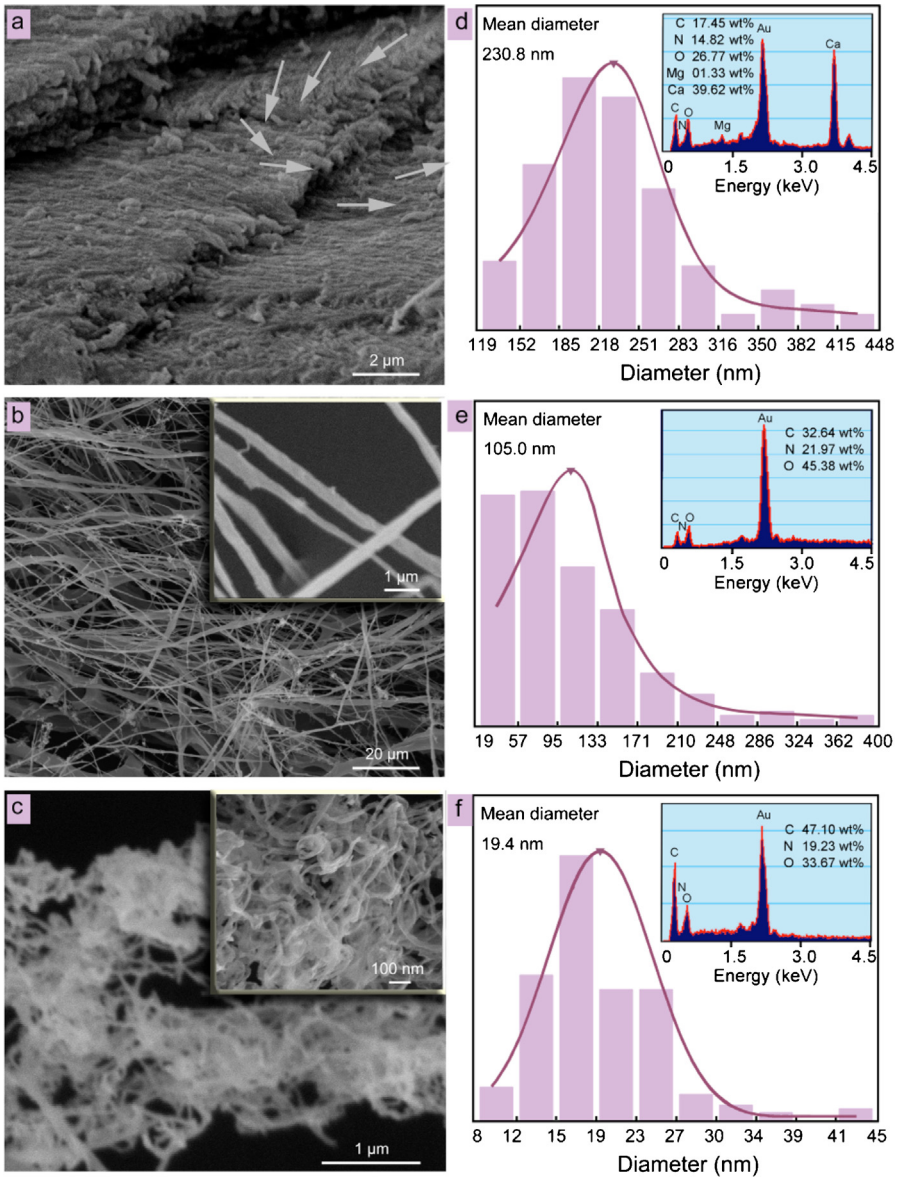

Fig. 2. SEM micrographs of (a) dry prawn shell without any purification, (b) after 5 min ultrasonication, and (c) after 30 min ultrasonication. The insets of SEM graphs are the amplifications. (d), (e), and (f) are the corresponding diameter distributions of the fibres of (a), (b), and (c), and insets are the EDS spectra.

film was immediately removed from the inner part of the dialysis membrane. The neat transparent film was obtained after drying in air.

The water suspension without dialysis was also obtained by the same process as the chitin hydrogels. Firstly, the origin suspension was poured into moulds and then placed in a refrigerator at −55 °C. Next, the frozen samples were subjected to freeze-drying using a Scientz-10N freeze-dryer (BT6K-ES, Virtis) to produce ice in the materials to sublime directly from the solid phase to the gas phase. The cold trap temperature was below −65 °C and the vacuum pressure was below 25 μPa during the freeze-drying process. The sonofibrillated chitin samples were obtained and used for characterisation.

2.5. Characterisation

The EDS spectra and SEM images were recorded on an FEI Quanta 200 SEM-EDS (EDS/EDX Genesis, EDAX Inc.), where the SEM was equipped with elemental analysis capabilities. The SEM images were obtained using an auto fine coater (JFC-1600; JEOL Ltd.) to coat the samples with gold to improve the conductivity.

The XRD patterns of the raw materials and the corresponding chitin nanofibers were measured with an XRD (D/max 2200, Rigaku) instrument using Ni-filtered Cu Kα radiation (λ = 1.5406 Å) at 40 kV and 30 mA. Scattered radiation was detected in the range $2\theta = 5°–40°$ at a scanning rate of 4°/min. The precision and accuracy of the diffraction peak positions were resolved from the diffraction spectra of raw materials and products using PeakFit® (Sea-Solve Software Inc., Richmond, CA) to evaluate the suitability of such a method to identify aspects of the chitin's crystalline structure not readily apparent in its diffraction spectrum (Cárdenas, Cabrera, Taboada, & Miranda, 2004). The crystallinity index (Cr_I) is obtained as the ratio of the area arising from the crystalline phase to the total area (Park, Baker, Himmel, Parilla, & Johnson, 2010).

The FTIR spectra were recorded on a Fourier transform infrared instrument (Magna 560, Nicolet, Thermo Electron Corp) in the range 400–4000 cm^{-1} with a resolution of 4 cm^{-1}. All the raw material and dry samples were ground into powder by a fibre microtome

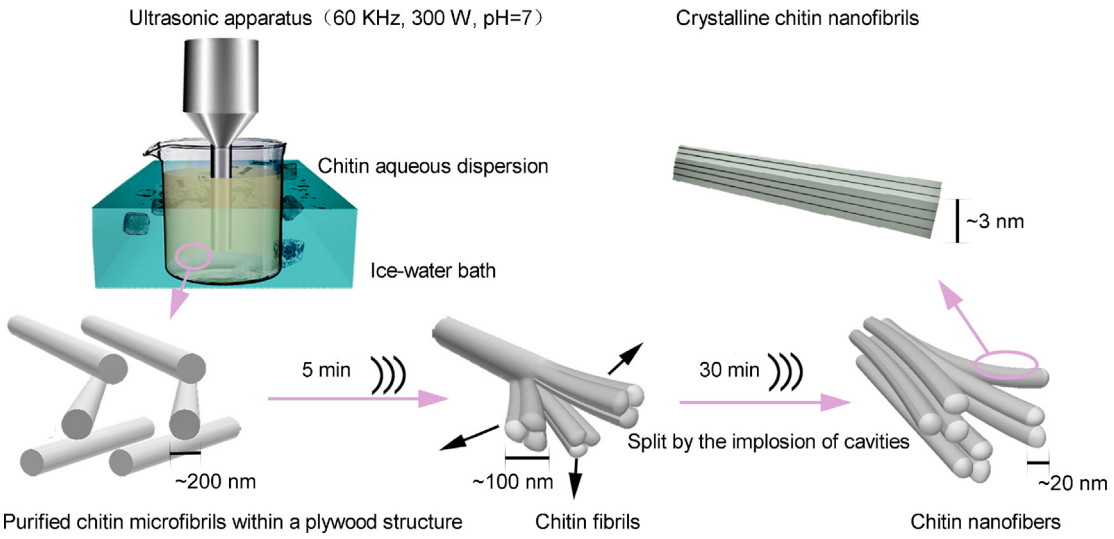

Fig. 3. The individualisation of α-chitin nanofibers from prawn shells with a typical laboratory-scale ultrasonication apparatus under neutral condition. The purified chitin microfibrils with the diameter of ~200 nm form the typical twisted plywood structure of the cuticle, and first split to thinner chitin fibrils after 5 min ultrasonic treatment along the axes of the fibres. All these chitin fibrils are further separated to 20 nm width nanofibers, which are aggregated by α-chitin nanofibrils. Each crystalline nanofibril contains 18–25 chitin molecules.

and then blended with KBr before pressing the mixture into ultrathin pellets.

The chitin nanofibril dispersion was introduced into a quartz cuvette, and the transmittance was measured from 300 to 800 nm using a UV–vis spectrophotometer (UV-1800, Shinadzu Corp., Japan). The spectrum of a cuvette filled with deionised water was used as a reference to correct the transmittance.

3. Results and discussion

3.1. Preparation of chitin nanofibers

Fig. 2a shows the microstructure of the black tiger prawn (*Penaeus monodon*) used as an arthropod cuticle model. Apparently, the bundled chitin microfibrils are helicoidally stacked, and the mean diameter of these original bundles is ~231 nm (Fig. 2d). Rich Ca (39.63 wt%) and few Mg (1.33 wt%) were detected in unpurified prawn shell, which was verified by its EDS spectrum (inset in Fig. 2d). Fig. 2b and c shows SEM images of the sample after 5 and 30 min of ultrasonic treatment, respectively, yielding plentiful slender fibrils with diameters of ~105 and ~20 nm. The bundled chitin microfibrils were disintegrated to the nanoscale in the ultrasonication process, and diameter of the separated chitin nanofibrils decreased with increasing ultrasonic treatment time. Additionally, the peaks of Ca and Mg disappeared in the EDS spectra of the samples (insets in Fig. 2e and f), indicating that the matrix substances (proteins and minerals) had been completely removed during the ultrasonic treatment process.

As shown in Figs. 1 and 3, the exoskeletons of crustaceans have a strictly hierarchical organisation, consisting of crystalline-chitin nanofibers as well as various proteins and minerals (Ifuku et al., 2009). The lowest molecular level was the chitin itself, the acetyl glucosamine monomer. Approximately 18–25 chitin molecules were aligned in an antiparallel manner, exhibiting the orthorhombic form that comprises α-chitin crystals in the form of thinner nanofibrils of approximately 3 nm in diameter. These crystalline chitin nanofibrils were wrapped in protein layers to form 5 to 50-nm-thick chitin–protein nanofibers, which can be regarded as the third level of the structural hierarchy. The next level in the scale consisted of the clustering of some of these nanofibers into chitin–protein fibrils of approximately 50–300 nm in diameter. The fifth level was the formation of a planar woven and plywood structure with a 180° helical twist (Fig. 2a) (Bouligand, 1972; Giraud-Guille & Besseau, 1998; Watthanaphanit & Addadi, 1997). Each hierarchical level of chitin–protein fibres was combined with inorganic nanoparticles, which mainly consisted of amorphous calcium carbonate, amorphous calcium phosphate, and Mg-calcite (Boßelmann, Romano, Fabritius, Raabe, & Epple, 2007; Raabe et al., 2006). The original chitin nanofibers were encased in embedding matrix components, and the crustacean cuticle was a natural hierarchical composite material. The fabricated nanofibers were the purified chitin nanofibers of the third hierarchical level.

In the ultrasonication process, the chitin component was firstly extracted from the prawn shell after chemical purification (including decolourisation, deproteination, and demineralisation). As shown in Fig. 3, the purified chitin suspension with a concentration of 0.5 wt% was passed through an ultrasonic processor for nano-fibrillation. This strategy is based on an ultra-sonication mechanism: ultra-sonication causes the natural fibres to disassemble into nanofibers in water *via* cavitation, formation, growth, and implosive collapse of bubbles in the solution. For instance, small gas bubbles (cavities) will be generated in a chitin aqueous suspension when the suspension is treated by ultrasound. These small gas bubbles are able to absorb energy from the sound waves and grow rapidly under high ultrasound intensities. However, the cavity implodes when the cavity has overgrown, and the surrounding liquid rushes in. The implosion of the cavity creates an unusual environment and introduces high-pressure and shock waves within a short time. This violent collapse causes direct particle-shock wave interactions (Zeiger & Suslick, 2011) and is the primary pathway to split chitin fibres along the axial direction. Thus, the sonification impact breaks the relatively weak chitin interfibrillar hydrogen bonding and the Van der Waals force, gradually disintegrating the micro-scale chitin fibres into nanofibers (Zhao et al., 2007).

This physical individualised method was also utilised to process commercial practical-grade chitin (PG-chitin), where the chitin microfibrils are composed of bundles of assembled nanofibers. Similar chitin nanofibers with a homogeneous width of ~20 nm were also obtained after 30 min of ultrasonic treatment (Fig. S1

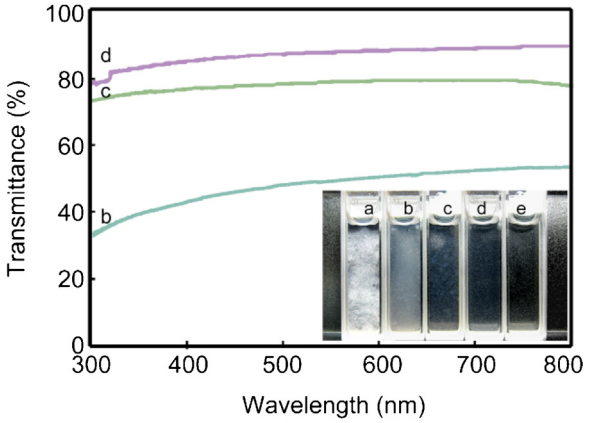

Fig. 4. Photographs and UV–vis spectra of dispersions of (a) chemical purified 0.5 wt% wet samples, (b) 0.5 wt% chitin dispersion after 5 min ultrasonication, (c) after 20 min processing, (d) nanofibrilised chitin nanofibers (0.5 wt%) after 30 min ultrasonication, and (e) the deionised water.

in the supplementary data). The ultrasonic treatment method is an efficient pathway to prepare ultrafine nanofibrils from chitin microfibers.

The obtained chitin nanofibrils were dispersed into deionised water (0.5 wt%), and their UV–vis spectra are displayed in Fig. 4. After simple chemical purification, the chitin nanofibrils were more apt to precipitate at the bottom of the bottle rather than to disperse well in water (bottle a in the inset of Fig. 4). When the sample was treated *via* 300 W ultrasonic pulses for 5 min, the obtained nanofibrils could disperse into deionised water (bottle b in the inset of Fig. 4). However, its transmittance was very low in the range 300–800 nm. For instance, the transmittance of the turbid suspension at 600 nm was less than 45% (curve b in Fig. 4), indicating that an appreciable amount of the bundles or aggregates of the nanofibers was still present in the dispersion. When the ultrasonication process was extended to 20 min, the dispersion of the obtained nanofibrils became much clearer, and the transmittance at 600 nm was greater than 75% (curve c in Fig. 4). If the ultrasonication treatment was carried out for 30 min, a homogeneous dispersion of chitin nanofibrils in water could be obtained, and the transmittance of the dispersion was as high as 89% in the range of visible light (curve d in Fig. 4). Clearly, ultrasonication treatment can disassemble the aggregated chitin nanofibrils to form a transparent and viscous chitin nanofibers dispersion in water.

3.2. Characterisation of chitin nanofibers

Fig. 5a shows the normalised FT-IR spectra of the dried prawn shell powder derived from black tiger prawn without purification and the newly prepared chitin nanofibers with different ultrasonic processing times obtained from prawn shell by removing the matrix components. For comparison, the spectrum of commercial PG-chitin was provided (Fig. S2 in supplementary data). Apparently, the spectrum of the dried prawn shell powder is very different from that of the newly prepared chitin nanofibers, which are consistent with the spectrum of the commercial PG-chitin. First, the absorption band at 1398 cm^{-1} disappears after the ultrasonication treatment. Given that this absorption band is assigned to protein, this disappearance suggests that the ultrasonication treatment has completely eliminated all the proteins. Furthermore, the characteristic absorption peaks from chitin nanofibers are summarised in Table 1. (Cárdenas et al., 2004; Muzzarelli et al., 2007; Naumann, Barnickel, Bradaczek, Labischinski, & Giesbrecht, 1982; Sdrobis et al., 2012; Sikorski, Hori, & Wada, 2009; Yamaguchi, Nge, Takemura, Hori, & Ono, 2005). The hydrogen bonds in α-chitin

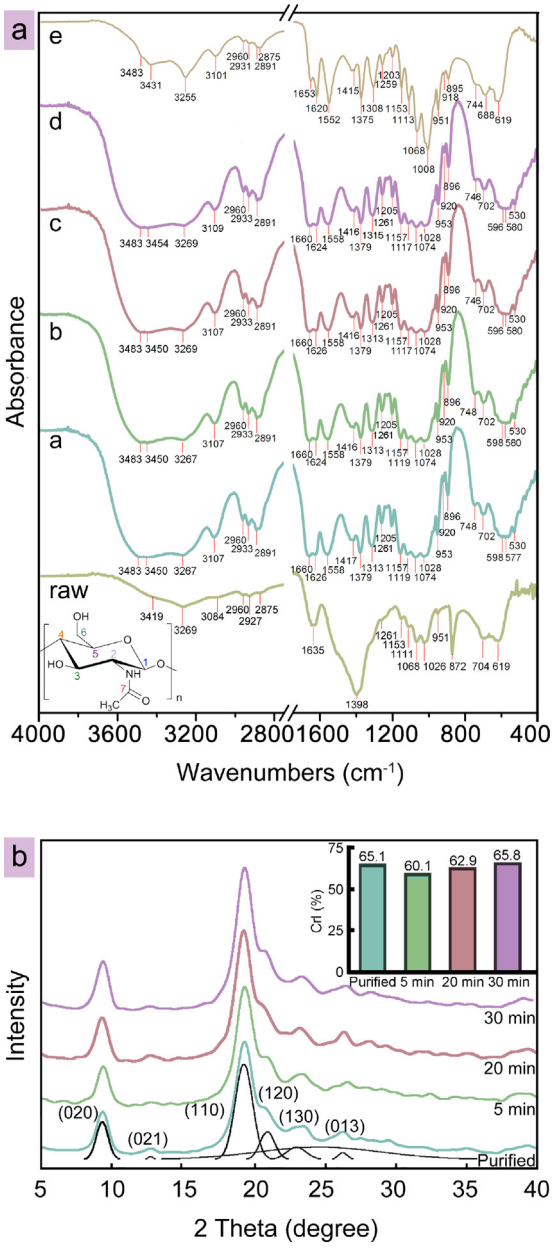

Fig. 5. (a) FT-IR spectra of dried pawn shell powder as the raw material without purification, a. chemical purified chitin samples from prawn shell, b. after 5 min ultrasonication, c. after 20 min processing, d. nanofibrillated chitin after 30 min ultrasonication, and e. dry PG-chitin commercially pre-purified from crustacea exoskeletons. (b) X-ray diffraction profiles of chemical purified chitin from prawn shell, sonofibrillated samples after 5 min, 20 min, and 30 min individually. The inset of (b) shows the corresponding crystallinity.

crystal structure are as follows, C(3)OH groups are intramolecular hydrogen-bonded to O(5) and C(6)OH (3450 cm^{-1} and 3483 cm^{-1}); C(6)OH groups are intermolecular hydrogen-bonded to the adjacent C(6)OH groups (3269 cm^{-1}); and half of C(6)OH groups are intermolecular hydrogen-bonded to C=O at the same time (1624 cm^{-1}). The C=O groups are also hydrogen-bonded to NH of the next parallel chitin chain (1660 cm^{-1}). These strong absorption peaks in the carbonyl region are especially characteristic of anhydrous α-chitin (Gopalan Nair & Dufresne, 2003). Besides the amide I (C=O stretching) split peaks and the O–H stretching peaks, the presence of pure α-chitin nanofibers is confirmed by the NH stretching band at 3269 cm^{-1}, the amide II band at 1558 cm^{-1}, and the amide II band at 1313 cm^{-1}. Amide II and amide III in

Table 1
Frequencies (cm^{-1}) of the main signals of α-chitin nanofibers from prawn shells and the assignments.

Absorption band (cm^{-1})	Assignment
3483	O(6)—H···O(3) stretch (intramolecular hydrogen-bonded)
3450	O(3)—H···O(5) stretch (intramolecular hydrogen-bonded)
3269	N—H stretch (asymmetric, Amide A) and O(6)—H···O(6) stretch (intermolecular hydrogen-bonded)
3107	N—H stretch (symmetric, Amide B)
2960	CH_3 stretch (asymmetric)
2933	CH_2 stretch (symmetric)
2878, 2891	C—H stretch
1660, 1624	C=O stretch (Amide I, N—H···O(7′)=C and O(6)—H···O(7′)=C bifurcate intermolecular hydrogen-bonded)
1558	C(2)—N stretch and N—H deformation in the CONH plane (Amide II)
1416	C—H deformation (asymmetric)
1379	C—H bending and CH_3 deformation (symmetric)
1313	C(2)—N stretch and N—H deformation (Amide III), CH_2 wagging
1261	N—H deformation (Amide IV)
1205	O—H in-plane bending and C—O stretch (symmetric)
1157	C(1)—O—C(4) stretch (bridge oxygen of glycosidic linkage, asymmetric)
1117	C(1)—O—C(5) stretch (in-plane glucose ring, asymmetric)
1074	C(3)—OH stretch
1028	C(6)—OH stretch
953	CH_3 wagging
920	CH_3 rocking
896	C(1)—H out-of-plane bending (Glucose ring, β bond)
746	CH_2 rocking
702	N—H out-of-plane bending (Amide V)
598	C—O out-of-plane bending
580, 530	C—C out-of-plane bending

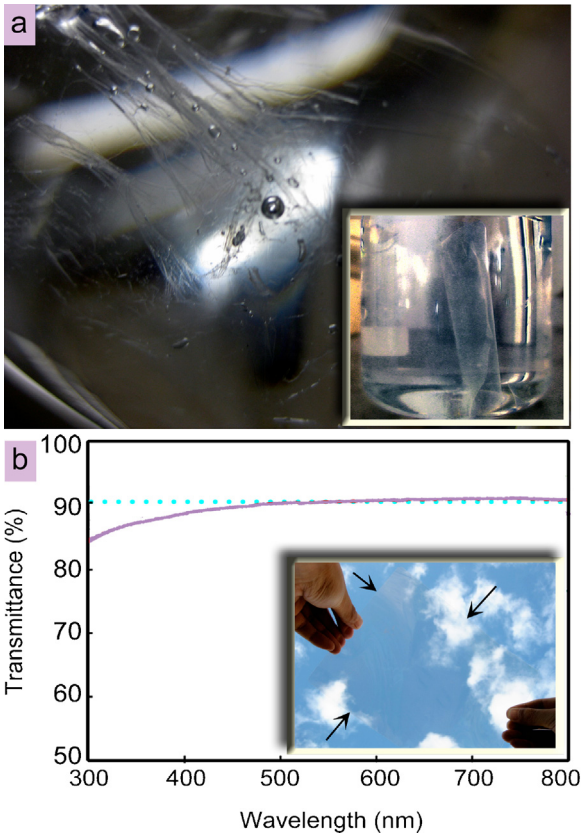

Fig. 6. (a) Image of wet large transparent neat chitin film, which is composed by chitin nanofibers with uniform diameters, the inset showed the film in a beaker. (b) The UV–vis transmittance spectra of dry chitin film. Inset is the appearance of dried optically transparent chitin film.

chitin correspond to the —NH bending modes mixed with the —CN stretching mode for the chitin nanofibers (Jin et al., 2013).

To obtain the crystallinity of the samples and analyse the effect of ultrasonic treatment on the reorganisation of chitin nanofibrils, an XRD study was carried out. Fig. 5b shows the diffractograms of sonofibrillated chitin samples with different processing times and the chemical purified prawn shell powder without nanofibrillation. The diffraction peaks of all chitin samples were observed at 9.3°, 12.8°, 19.3°, 20.9°, 23.4°, and 26.2°, which corresponded to the planes of (0 2 0), (1 0 1), (1 1 0), (1 2 0), (1 3 0), and (0 1 3), respectively. The diffraction peak at 29.6° is completely absent from all the normalised X-ray diffraction profiles; this peak is characteristic of calcium carbonate, indicating that the mineral component was thoroughly removed during the demineralised procession. The crystallinity of sonofibrillated chitin samples (Cr_I = 60–66) changed little with the chemical purified shell powder (Cr_I = 65.1) because the crystalline chitin nanofibrils (second hierarchical level) were essentially unchanged by the sonification. The diffraction profile of the chitin nanofibers is highly similar to that of purified shell powder, indicating that the crystal structure of the obtained nanofibers did not change significantly after 30 min of ultrasonication. Thus, the original molecular structure and chitin crystalline structure were substantially maintained even after the removal of the matrix and the ultrasonic treatments. Furthermore, the result shows that the adding time of ultrasonic application increase the crystallinity degree of chitin fibres (inset of Fig. 5b). The Cr_I of the sample even higher than the starting material after 30 min sonication. The same phenomenon was also observed of the ultrasonic treated bacterial cellulose (Tischer et al., 2010). It can be concluded that the ultrasound energy may transfer through cavitation and promoted the recombination of molecular chains. The energy scale of the cavitation processes is within the hydrogen bond energy scale and occurs primarily in the amorphous regions, where water can more effectively penetrate. While the process of fibre-splitting happened along the axial direction, the energy also fused the surface of neighbouring ribbons to convert amorphous region (less ordered chains) into crystalline (highly ordered chains) region (Shchukin, Skorb, Belova, & Möhwald, 2011).

3.3. *Fabrication of neat chitin nanofiber transparent film and flexible foam*

The transparent chitin aqueous suspension was kept in dialysis tubing for 48 h to obtain a transparent ultrathin film on the inner wall of the dialysis tube. This neat chitin film could be removed by soaking in water, and the film remained highly transparent in water (Fig. 6a), suggested that the film was applicable for underwater tasks. The inset of Fig. 6b showed the appearance of a dried, optically transparent chitin film after oven drying and die-cutting. The light transmittance spectrum of the optically transparent neat chitin film prepared from nanofibrillated chitin is shown in Fig. 6b. The fully fibre-made film had high transparency in the visible light range (300–800 nm), indicating that each chitin nanofiber was much thinner than the wavelength of visible light. Remarkably, the transmittance of the obtained film was 90.2% at a 600 nm, which is the centre of the visible light spectrum. These results indicate that the chitin nanofibers obtained from prawn shells can be fully fibrillated by ultrasonic treatment under neutral conditions.

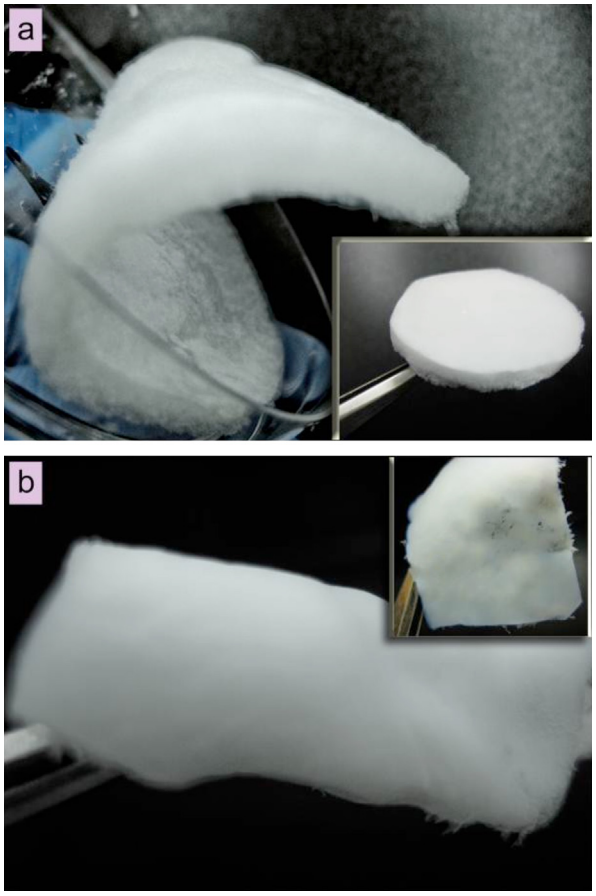

Fig. 7. Photographs of the soft foams made up by the long entangled chitin nanofibrils. (a) The freeze-dried round-like foam from the collected hydrogel, and (b) the freeze-dried square foam from the organogel after the solvent-exchanged with *t*-BuOH.

The condensed chitin nanofibril hydrogel was collected and subjected to solvent exchange with *t*-BuOH. After freeze-drying the hydrogel and organogel, high-flexibility and high-ductility chitin foams were fabricated. Fig. 7 shows the foams, which have a white appearance and a bulk density of 5×10^{-3} g cm^{-3} and can be repeatedly bent without destroying their structural integrity. Thus, the separated nanofibrils can be easily stored and transported.

These findings also verify that highly flexible and low-density nanofiber-foams containing chitin nanofibers have been successfully prepared. Such foams consisting of ultralong chitin fibres are expected to be used in various fundamental and applied fields, such as nanofiber templates for hollow inorganic tubes, tissue engineering scaffolds, filtration media, water purification, and packaging materials.

4. Conclusions

In summary, α-chitin nanofibers with a uniform width of approximately 20 nm were successfully prepared from dried prawn shell by high-intensity ultrasonication (300 W, 60 KHz, 30 min) nanofibrillation after chemical purification (including decolourisation, deproteination, and demineralisation). The ultrasonication process, used as a physical nanofibrillation technique, could disassemble the micro-scale fibres into nanofibers in water *via* cavitation. The shockwaves caused by the implosion of the cavity can break the relatively weak chitin interfibrillar hydrogen bonding and the Van der Waals forces to gradually form nanofibers. It is also observed that the pulsed ultrasonic treatment had the trend to improve the Cr_I of chitin. In this project, we also successfully adopt this physical individualised method to separate nanofibers from commercial PG-chitin. In addition, the present work also produced highly transparent films and soft foams with chitin nanofibers. Therefore, the developed nanofibers with a uniform width and high surface-to-volume ratio could be transformed into novel green functional materials. As a simple approach, the ultrasonic nanofibrillation method will be extended to the production of ultralong nanofibers from other natural polysaccharide materials. It is a new opportunity to fabricate novel nanomaterials from biomass materials, which is crucial for fully utilising abundant biomass resources.

Acknowledgement

This work was financially supported by The National Natural Science Foundation of China (31270590 and 21207073).

Appendix A. Supplementary data

Supplementary data associated with this article can be found, in the online version, at http://dx.doi.org/10.1016/j.carbpol.2013.07.038.

References

Abe, K., Iwamoto, S., & Yano, H. (2007). Obtaining cellulose nanofibers with a uniform width of 15 nm from wood. *Biomolecules*, *8*(10), 3276–3278.
Bang, J. H., & Suslick, K. S. (2010). Applications of ultrasound to the synthesis of nanostructured materials. *Advanced Materials*, *22*(10), 1039–1059.
Boßelmann, F., Romano, P., Fabritius, H., Raabe, D., & Epple, M. (2007). The composition of the exoskeleton of two crustacea: The American lobster *Homarus americanus* and the edible crab *Cancer pagurus*. *Thermochimica Acta*, *463*(1/2), 65–68.
Bouligand, Y. (1972). Twisted fibrous arrangements in biological materials and cholesteric mesophases. *Tissue and Cell*, *4*(2), 189–217.
Cárdenas, G., Cabrera, G., Taboada, E., & Miranda, S. P. (2004). Chitin characterization by SEM, FTIR, XRD, and ^{13}C cross polarization/mass angle spinning NMR. *Journal of Applied Polymer Science*, *93*(4), 1876–1885.
Chen, P.-Y., Lin, A. Y.-M., McKittrick, J., & Meyers, M. A. (2008). Structure and mechanical properties of crab exoskeletons. *Acta Biomaterialia*, *4*(3), 587–596.
Cheng, Q., Wang, S., & Han, Q. (2010). Novel process for isolating fibrils from cellulose fibers by high-intensity ultrasonication. II. Fibril characterization. *Journal of Applied Polymer Science*, *115*(5), 2756–2762.
Ding, B., Cai, J., Huang, J., Zhang, L., Chen, Y., Shi, X., et al. (2012). Facile preparation of robust and biocompatible chitin aerogels. *Journal of Materials Chemistry*, *22*(12), 5801–5809.
Fan, Y., Saito, T., & Isogai, A. (2010). Individual chitin nano-whiskers prepared from partially deacetylated α-chitin by fibril surface cationization. *Carbohydrate Polymers*, *79*(4), 1046–1051.
Giraud-Guille, M. M. (1984). Fine structure of the chitin–protein system in the crab cuticle. *Tissue and Cell*, *16*(1), 75–92.
Giraud-Guille, M.-M., & Besseau, L. (1998). Banded patterns in liquid crystalline phases of type I collagen: Relationship with crimp morphology in connective tissue architecture. *Connective Tissue Research*, *37*(3/4), 183–193.
Gopalan Nair, K., & Dufresne, A. (2003). Crab shell chitin whisker reinforced natural rubber nanocomposites. 1. Processing and swelling behavior. *Biomacromolecules*, *4*(3), 657–665.
Ifuku, S., & Saimoto, H. (2012). Chitin nanofibers: Preparations, modifications, and applications. *Nanoscale*, *4*(11), 3308–3318.
Ifuku, S., Nogi, M., Abe, K., Yoshioka, M., Morimoto, M., Saimoto, H., et al. (2009). Preparation of chitin nanofibers with a uniform width as α-chitin from crab shells. *Biomacromolecules*, *10*(6), 1584–1588.
Isogai, A., Saito, T., & Fukuzumi, H. (2011). TEMPO-oxidized cellulose nanofibers. *Nanoscale*, *3*(1), 71–85.
Jin, J., Hassanzadeh, P., Perotto, G., Sun, W., Brenckle, M. A., Kaplan, D., et al. (2013). A biomimetic composite from solution self-assembly of chitin nanofibers in a silk fibroin matrix. *Advanced Materials*, http://dx.doi.org/10.1002/adma.201301429
Lu, Y., Sun, Q., Yang, D., She, X., Yao, X., Zhu, G., et al. (2012). Fabrication of mesoporous lignocellulose aerogels from wood via cyclic liquid nitrogen freezing-thawing in ionic liquid solution. *Journal of Materials Chemistry*, *22*(27), 13548–13557.
Muzzarelli, R. A. A. (2009). Chitin and chitosans for the repair of wounded skin, nerve, cartilage and bone. *Carbohydrate Polymers*, *76*, 167–182.
Muzzarelli, R. A. A. (2011). Chitin nanostructures in living organisms. In S. N. Gupta (Ed.), *Chitin formation and diagenesis* (Vol. 34) (pp. 1–34). Dordrecht: Springer.
Muzzarelli, R. A. A., Muzzarelli, C., Cosani, A., & Terbojevich, M. (1999). 6-Oxychitins, novel hyaluronan-like polysaccharides obtained by regioselective oxidation of chitins. *Carbohydrate Polymers*, *39*, 361–367.

Muzzarelli, R. A. A., Morganti, P., Morganti, G., Palombo, P., Palombo, M., Biagini, G., et al. (2007). Chitin nanofibrils/chitosan glycolate composites as wound medicaments. *Carbohydrate Polymers*, *70*(3), 274–284.

Muzzarelli, R. A. A., Boudrant, J., Meyer, D., Manno, N., DeMarchis, M., & Paoletti, M. G. (2012). A tribute to Henri Braconnot, precursor of the carbohydrate polymers science, on the chitin bicentennial. *Carbohydrate Polymers*, *87*, 995–1012.

Naumann, D., Barnickel, G., Bradaczek, H., Labischinski, H., & Giesbrecht, P. (1982). Infrared spectroscopy, a tool for probing bacterial peptidoglycan potentialities of infrared spectroscopy for cell wall analytical studies and rejection of models based on crystalline chitin. *European Journal of Biochemistry*, *125*, 505–515.

Park, S., Baker, J. O., Himmel, M. E., Parilla, P. A., & Johnson, D. K. (2010). Cellulose crystallinity index: Measurement techniques and their impact on interpreting cellulase performance. *Biotechnology for Biofuels*, *3*, 1–10.

Qin, Y., Lu, X., Sun, N., & Rogers, R. D. (2010). Dissolution or extraction of crustacean shells using ionic liquids to obtain high molecular weight purified chitin and direct production of chitin films and fibers. *Green Chemistry*, *12*(6), 968–971.

Raabe, D., Romano, P., Sachs, C., Fabritius, H., Al-Sawalmih, A., Yi, S. B., et al. (2006). Microstructure and crystallographic texture of the chitin–protein network in the biological composite material of the exoskeleton of the lobster *Homarus americanus*. *Materials Science and Engineering A*, *421*(1/2), 143–153.

Sdrobis, A., Loanid, G. E., Tevanovic, T. S., & Vasile, C. (2012). Modification of cellulose/chitin mix fibers with N-isopropylacrylamide and poly(N-isopropylacrylamide) under cold plasma conditions. *Polymer International*, *61*, 1767–1777.

Shams, M. I., Ifuku, S., Nogi, M., Oku, T., & Yano, H. (2011). Fabrication of optically transparent chitin nanocomposites. *Applied Physics A*, *102*(2), 325–331.

Shchukin, D. G., Skorb, E., Belova, V., & Möhwald, H. (2011). Ultrasonic cavitation at solid surfaces. *Advanced Materials*, *23*, 1922–1934.

Sikorski, P., Hori, R., & Wada, M. (2009). Revisit of α-chitin crystal structure using high resolution X-ray diffraction data. *Biomacromolecules*, *10*(5), 1100–1105.

Suslick, K. S. (1990). Sonochemistry. *Science*, *247*(4949), 1439–1445.

Synowiecki, J., & Al-Khateeb, N. A. (2003). Production, properties, and some new applications of chitin and its derivatives. *Critical Reviews in Food Science and Nutrition*, *43*(2), 145–171.

Tischer, P. C. S. F., Sierakowski, M. R., Westfahl, H., & Tischer, C. A. (2010). Nanostructural reorganization of bacterial cellulose by ultrasonic treatment. *Biomacromolecules*, *11*(5), 1217–1224.

Watthanaphanit, S., & Addadi, L. (1997). Design strategies in mineralized biological materials. *Journal of Materials Chemistry*, *7*(5), 689–702.

Watthanaphanit, A., Supaphol, P., Tamura, H., Tokura, S., & Rujiravanit, R. (2008). Fabrication, structure, and properties of chitin whisker-reinforced alginate nanocomposite fibers. *Journal of Applied Polymer Science*, *110*(2), 890–899.

Yamaguchi, Y., Nge, T. T., Takemura, A., Hori, N., & Ono, H. (2005). Characterization of uniaxially aligned chitin film by 2D FT-IR spectroscopy. *Biomacromolecules*, *6*(4), 1941–1947.

Zeiger, B. W., & Suslick, K. S. (2011). Sonofragmentation of molecular crystals. *Journal of the American Chemical Society*, *133*(37), 14530–14533.

Zeng, J.-B., He, Y.-S., Li, S.-L., & Wang, Y.-Z. (2011). Chitin whiskers: An overview. *Biomacromolecules*, *13*(1), 1–11.

Zhao, H.-P., Feng, X.-Q., & Gao, H. (2007). Ultrasonic technique for extracting nanofibers from nature materials. *Applied Physics Letters*, *90*(7), 073112.